A PROPOSED COMMUTATION TECHNIQUE FOR SWITCHED-MODE SMART-POWER APPLICATIONS BASED ON V_{GS} SLEW-RATE ADJUSTING

Fernando C. Castaldo and Carlos Alberto dos Reis Filho
State University of Londrina-UEL and State University of Campinas-UNICAMP
castaldo@LPM.fee.unicamp.br and carlos_reis@LPM.fee.unicamp.br

***Abstract* - This paper introduces a controlling technique intended for Smart-Power applications where the EMI generated may be adjusted. The tradeoff between the EMI generation and switching losses are pinpointed and some considerations about radiated emissions are discussed. Finally, an integrated boost converter is shown to validate the previous analysis and some pre-compliance EMI measurements are carried out.**

KEYWORDS

Driving Techniques, Smart-Power, Switched Mode Applications.

INTRODUCTION

The conventional hard switching power MOSFET is widely employed in PWM controlled Smart-Power Applications considering its compatibility with CMOS process, which allows for the implementation of Applied Specific Integrated Circuits (ASICs) [1]. However, it is know that the hard switching generates high levels of electromagnetic noise (EMI) along with commutation losses. Soft-switching techniques which reduces both the EMI and the switching losses requires the use of discrete resonant elements for achieving either the Zero-Current-Commutation (ZCS) or the Zero-Voltage-Commutation (ZVS), being not suitable for ASICs implementation [2]. Other techniques are based on driver strategies that speed-up the commutation process without generating high levels of EMI. The snubber-less gate driving technique based on different current paths for both charging and discharging the transistor's input capacitance aided by current/sink generators have been claimed to be a good compromise between EMI generated and switching losses [3], [4]. Moreover, Multi-Gate-Resistor driver can optimize the more appropriate configuration for turning on and off the main transistor aiming the reduction of commutation intervals, experiencing some EMI reduction by shaping the gate current [5]. These drivers can be digitally controlled, a feature suitable for integration [6], [7]. Nevertheless, all these approaches do not have the ability of continuously adjusting the EMI level generated by the switching process.

V_{GS} SLEW-RATE ADJUSTING TECHNIQUE

The power MOSFET driving technique based upon the V_{GS} slew-rate adjusting can reduce the EMI levels generated by the switching operation, as proposed in this paper. Thus, it is presented a PWM driver that generates an output voltage with both the rising and falling edge control feature. Experimental results have shown that the technique can control efficiently the EMI generated. However, there is some increase of the switching losses due to the increase of the commutation intervals [8]. Therefore, the higher the switching losses, the lower the EMI generated and vice-versa, so a tradeoff between switching losses and generated EMI can be established in order to optimize the application's performance.

To illustrate the technique, the circuit in Fig.1(a) is used to model the transistor driving a classical inductive load along with the clamping diode. The driver that controls the power transistor has an output impedance represented by R_G. Fig. 1(b) shows the linear transistor model that the commutation analysis is deduced from [9].

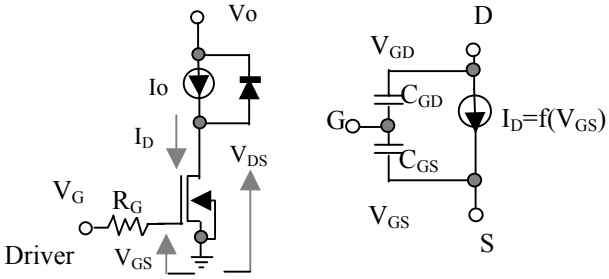

Fig. 1 (a) Basic Circuit (b) Transistor Model

Fig. 2 shows the basic waveforms for the circuit of Fig. 1(a) [10]. A V_G output driver PWM signal with duty cycle D, period T and variable slew-rate is close to the voltage V_{GS} if the driver output impedance R_G is supposed to be low enough. As indicated, the variable slew-rate V_{GS} can control the voltage V_{DS} and current I_D commutation intervals by speeding them up or down. Doing so, the dissipated power due to the switching process can be adjusted and so can the EMI levels generated.

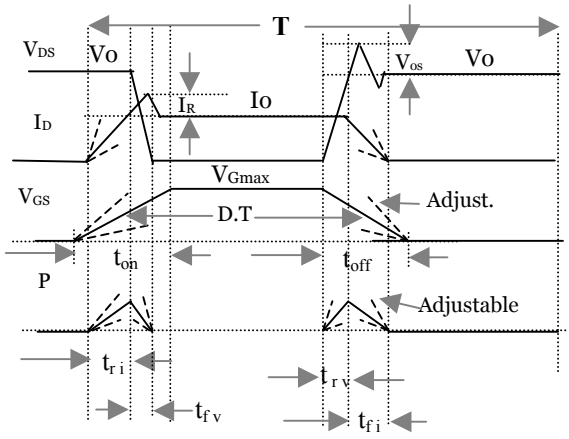

Fig. 2 Transistor waveforms for an inductive load and variable slew-rate

An important characteristic should be considered here: As Smart-Power Applications are supposed to be integrated, a driving strategy can be developed and easily implemented on the low-power controlling side. All the switching characteristics will be controlled by V_{GS} applied voltage. Thus, specific ASICs can be developed aiming the real time optimization of the tradeoff between EMI and switching losses based on both V_{GS} slew-rate control and electromagnetic emissions sensing circuits. Therefore, neither auxiliary circuits nor snubbers will be used in this approach in order to feature the commutation technique.

EMI CONSIDERATIONS

The main purpose by which adjusted slew-rate gate driving applies is to keep the EMI levels under desirable values, according the EMI/EMC standards. When dealing with switched mode applications (SMA) in EMI realm, either low or high power, the same issues apply, e.g. reverse current of switching diodes that will generate high frequency noise or the presence of stray inductances that will produce ringing and over-voltages, also accounting for the levels of total generated EMI. The diode reverse current is a fast transient that generates high frequency magnetic fields. These in turn couple another parts of the circuit and induce common mode voltages that can propagate through the circuit [11]. The other hand, the ringing associated with the blocking action of the transistor is due to the energy stored in stray inductance that may cause over-voltages if not suitable clamped. The electric field associated can also propagate as well [12]. The main level of EMI generated in a SMA is due these primary mechanisms. The higher the amplitude of switched current and voltage (and their time derivatives), the more the EMI generated levels. According [5], Eq. 1 calculates the diode reverse current and the drain-to-source over-voltage. See Fig. 2.

$$I_R = \sqrt{2 \cdot \tau \cdot I_o \cdot \frac{d}{dt} I_{Don}} \qquad V_{os} = L_S \cdot \frac{d}{dt} I_{Doff} \tag{1}$$

The new parameters are the stray inductance L_S placed along the DC supply and the power transistor, the mean lifetime carrier of the diode τ, the transistor turn-on drain current I_{Don} and the transistor turn-off current I_{Doff} Both derivatives are V_{GS} controlled. From Eq. 1 is clear that these undesirable effects can be attenuated however not completely eliminated. It is implied that the V_{GS} slew-rate adjusting can reduce these derivatives and therefore the EMI levels. In the proposed technique the more appropriate slew-rate to be applied is chosen based on emissions tests aiming the application circuit to be operated with both reduced thermal stress and electromagnetic emission.

EVALUATION OF THE TECHNIQUE IN AN INTEGRATED BOOST CONVERTER APPLICATION

In order to illustrate the proposed driving technique a PWM switched mode low power boost circuit operating in CCM-continuous conduction mode is presented [10]. A Boost converter with active elements integrated was designed using CMOS process 0,8µ technology. Only resistors and some capacitors were used externally. The slew-rate controller driver was also integrated along with the PWM circuit generator and auxiliary circuits. The switching power transistor is known as LDD (Light Doped Drain) High Voltage transistor. Other parameters of the transistor are also related: β=0,46A/V^2; C_{GD}=47pF; C_{GS}=844pF [13]. The output driver impedance is considered R_G=10Ω obtained by means of simulations. The magnetic element is a small RF inductor of 100µH placed externally. The boost converter is designed to operate at a 600KHz, 300mA full load current, output voltage 12V, input voltage 5V. See Fig. 3.

In the proposed test, V_{DS} and I_D are monitored for some values of V_{GS} slew-rates and the spectra are measured in order to check out the EMI levels. The spectrum measurement procedure uses a near magnetic field probe and the measurements are relative to dBµV in spite of the 50Ω spectrum analyzer impedance [18].

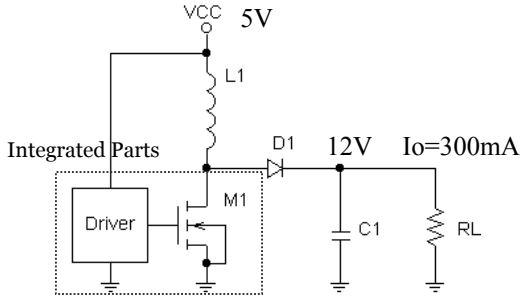

Fig. 3 Switched Mode Application: Boost Circuit

The adjustable slew-rate driver is shown in Fig. 4. It is based on the controlled charge and discharge of an integrated capacitor by means of dependent current sources.

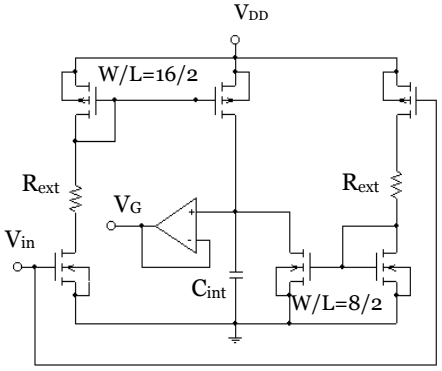

Fig. 4 Adjustable Slew-Rate Driver

External variable resistors were used for adjusting the rise and fall times. However, in a fully integrated version, these resistors can be replaced by controlled current sources, allowing some degree of automatic control.

Fig. 5 shows the main waveforms for the converter when operating under two different V_{GS} slew-rates, (a) 0,125V/ns (t_{on}=t_{off}=40ns, see Fig. 2) and (b) 0,011V/ns (t_{on}=t_{off}=450ns). The duty cycle is nearly 40% and the both rising and falling slew-rates were kept the same for simplifying reasons. A shunt resistor of 1Ω was used in order to read the drain current. Note that in case (a) the fast ringing on voltage and

current waveforms due the already cited mechanisms. Case (b) takes advantage of reduced EMI levels.

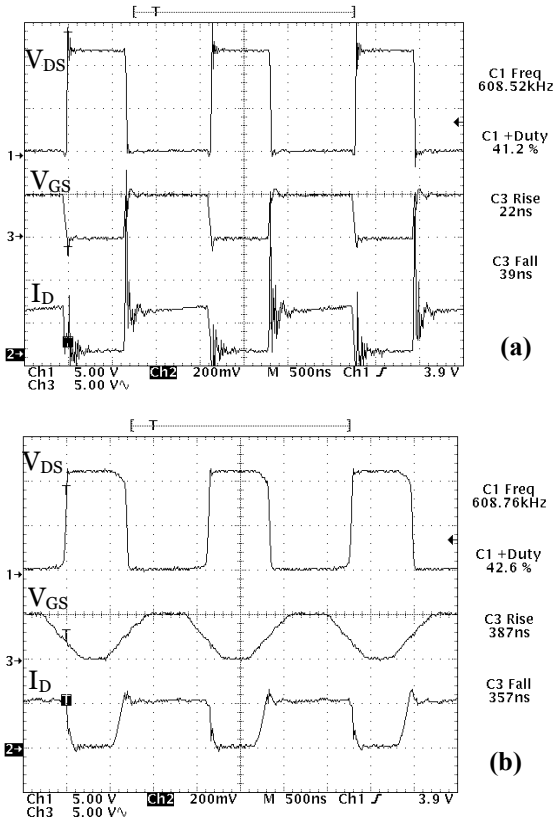

Fig. 5 Boost Converter Main Waveforms

Fig. 6 shows the spectra measured by the magnetic field probe for the cases (a) and (b) as indicated in Fig. 5. Note that there is almost a reduction of -20dB on near irradiated magnetic field, when the power transistor is driven by the slower slew-rate.

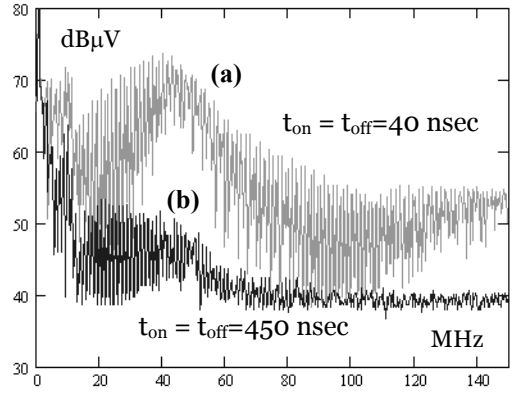

Fig. 6 Near Magnetic Field Spectrum

A simplified expression to estimate the commutation losses as a function of the applied V_{GS} slew-rate was developed based on the commutation intervals calculations [8], [9] and the MOSFET transistor operating in saturation region [14]. The result is given in Eq. 2.

$$P = \frac{1}{2}\cdot I_O \cdot V_O \cdot \left[\sqrt{2\cdot Vo\cdot R_G \cdot C_{GD}}\cdot\left(\frac{1}{\sqrt{TS}}+\frac{1}{\sqrt{TF}}\right)+\right.$$
$$\left.+\sqrt{\frac{I_O}{\beta}}\cdot\left(\frac{1}{TS}+\frac{1}{TF}\right)\right]\cdot f_s \qquad (2)$$

Referring to Fig. 2, the slew-rate parameters are the V_{GS} rising edge slew-rate ($T_S = V_{Gmax} / t_{on}$) and the falling one ($T_F = V_{Gmax} / t_{off}$). The switching frequency is the inverse of the period T (f_s=1/T). The MOS transconductance parameter is given by $\beta=(K_N/2).(W/L)$ where K_N is the transconductance transistor parameter, W and L the width and length of the transistor respectively. R_G and C_{GD} were already mentioned.

The losses due to the switching process were estimated based on the transition intervals measurements from oscilloscope cursor feature and compared with the calculated values. Thus for C_{GD}=47pF, β=0,46A/V^2, R_G=10Ω, Io=300mA, Vo=12V, $T_S=T_F$ and V_{Gmax}=5V, Tab.1 shows the calculated and measured average power dissipation due to the commutation losses as function of the V_{GS} slew-rate T_S,T_F, given in terms of t_{on} and t_{off}.

TABLE I
Switching Losses

$t_{on}=t_{off}$ (n sec)	Measured (mW)	Calculated (mW)
100	40	38
200	86	64
300	111	87
400	142	118
500	169	143

In order to evaluate Eq. 2, a simplified transistor model was used, as indicated in Fig. 1. Referring to this model, the C_{GD} capacitance was considered constant and given by the sidewall capacitance value [14]. The *Miller effect* [3] was not taken into account.

ESTIMATION OF THE FAR-ELECTRIC-FIELD PRE-COMPLIANCE TESTS

EMI/EMC Standards are applied for any equipment be marketed in a place. These standards are regulated by governmental agencies that set the limit of electromagnetic emission allowable for electronic equipments [15]. The certification of a product should be based on tests of electromagnetic emissions using specific sites, known as anechoic chambers or even in open site, which are expensive tests and normally used for final certification of compliance. However, in a step design or prototyping, the engineer is able to check the emission level of a circuit under development. To do so, one can employ the near magnetic field measurement. This method works as detector for emissions leakage, but the relative imprecision of the relationship between near and far fields can mask some results [16]. The measurement of far fields using a basic setup outside an anechoic chamber would imply in several errors of measurements and therefore would give only a slight idea of how far the compliance to be reached is. This procedure

saves time and money because countermeasures can be taken in design step instead of applying remedies to final products [17].

In this work, a basic setup composed by a spectrum analyzer and a bi-conical calibrated antenna was used to perform the checkout of the boost converter with EMI adjust feature. First of all, a basic calibration was carried out in order to determine the environmental background noise, which was subtracted from the actual measurements to give a relative clean reading. Next, the circuit was placed 1m away from the antenna and only plane wave radiating fields were considered to propagate. It is worth to say that this procedure is to check out the slew-rate adjusting feature instead of measuring actual emissions and a tolerance of 6dB is usual in common practice. A shift rule was applied to correlate the 10m measuring distance from CISPR 22 standard and the actual 1m-distance measurement [18]. The spectrum analyzer was set in peak-detection mode with a resolution bandwidth of 120KHz. The frequency range was chosen starting from 10MHz up to 150MHz. Only horizontal polarization was considered and losses cables were not taken into account. The next graphs show the measured electric fields as function of the slew-rate adjusting for (a) 0,125V/ns (t_{on}=t_{off}=40ns) and (b) 0,011V/ns (t_{on}=t_{off}=450ns). The slower the V_{GS} transitions, the less the emissions will be.

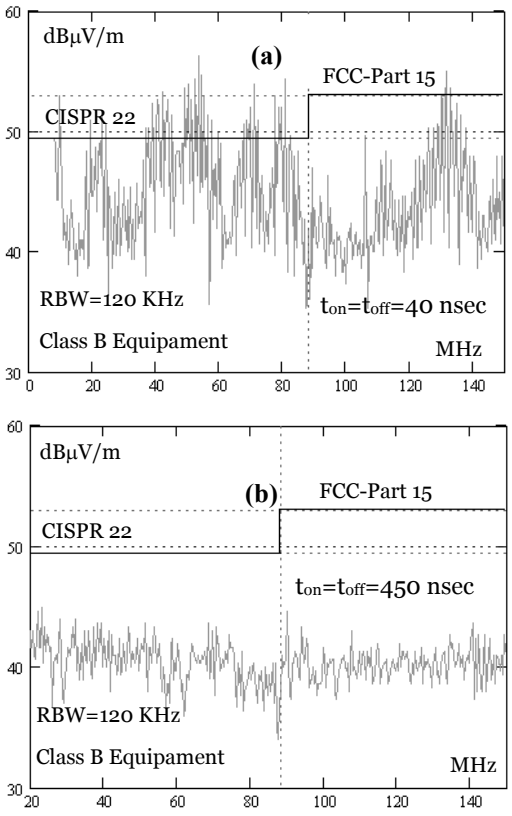

Fig. 7 1m-Electric Field Measurement

(a) t_{on}= t_{off}= 40 nsec (b) t_{on}= t_{off}= 450 nsec

Fig. 7 shows that it is not necessary to choose such low slew-rates because the limit imposed by regulation is far above the actual emissions and benefits from lower switching losses can be achieved if a faster slew-rate is chosen. However, the design engineer should take into account the tolerance to errors of such approach and work with relatively greater values if the final version of a product is to be compliant with the regulation.

IC MICROPHOTOGRAPHY AND BASIC MEASUREMENT SETUP

Fig. 8 shows the microphotography of the integrated circuit. One can note the power MOSFET transistor split in two. Other structures are also integrated as PWM generator, drivers and current sources.

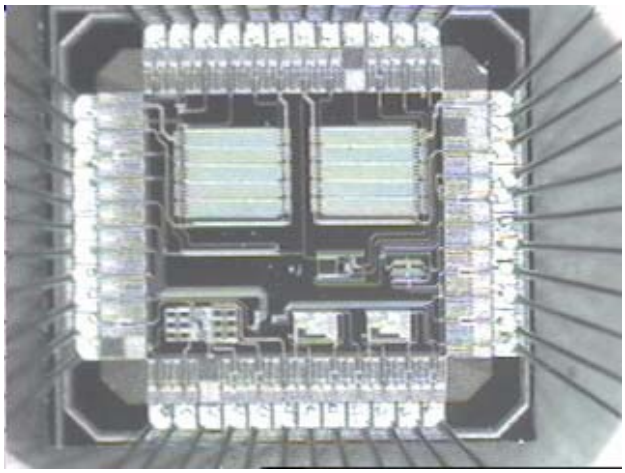

Fig. 8 IC Microphotography

Fig. 9 shows the antenna setup placed 1m away from the SMA boost converter in order to check out the EMI levels measured in terms of electric field.

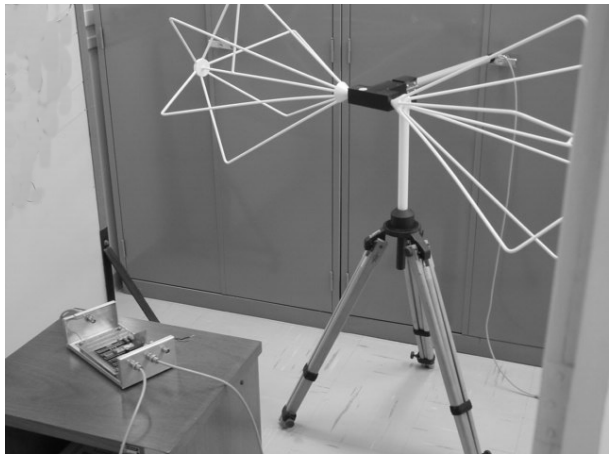

Fig. 9 Basic Antenna Setup and Electric Field Measurement

Fig 10 shows the complete circuit, along with the auxiliary passive components. Also can be seen the loop probe for near magnetic field measurements.

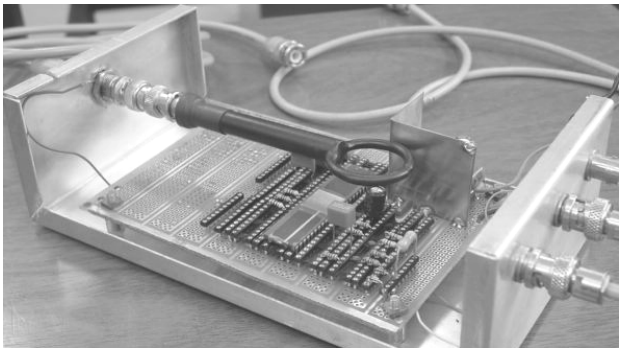

Fig. 10 Near Field Measurement and Probe Loop

CONCLUSIONS

In this paper, a MOSFET driving technique is proposed aiming the reduction of the EMI problem. This technique is suitable for Switched Mode Smart-Power applications with EMI controlling feature allowing for the implementation of both optimized drivers and low electromagnetic emissions ASICs. A simplified model for commutation losses is proposed and the tradeoff between switching losses and EMI is discussed. Finally, some experimental results from an integrated boost converter with EMI level adjusting feature is presented along with some basic emissions tests for pre-compliance estimation.

REFERENCES

[1] Murari, B. et al. *Smart Power Ics.* Springer-Verlag. ISBN: 3-540-60332-8.

[2] Qian J., Bruning. G. 2.65 MHz High efficiency soft-switching power amplifier system Power Electronics Specialists Conference, 1999. PESC 99. 30th Annual IEEE , pp 370 –375 vol.1.

[3]Galuzzo, A et al. Switching characteristics improvement of modern gate controlled devices. Power Electronics and Applications, 1993. Fifth European Conference pp: 374 -379 vol.2

[4] Musumeci, S. et al. Switching behavior improvement of insulated gate controlled devices. Power Electronics, IEEE Transactions on, Vol Jul 1997 pp. 645 -653

[5] Sachdeva, R. Nowick, E.P. Characterization of a gate drive technique for snubberless operation of gate controlled devices. Electrical and Computer Engineering, 2001. Canadian Conference on, 2001 pp: 1085 –1089 vol.2.

[6] Yamada, A Matsumoto, K. A high voltage intelligent module (HVIPM) with a high performance gate driver. Power Semiconductor Devices and ICs, ISPSD 98. Proceedings of the 10th International Symposium on, 1998 pp. 289 -292.

[7] Kim, E.D. et al. An intelligent power module for IGBT gate driver implemented in 0,8um high voltage CMOS process. Industrial Electronics, 2001. Proceedings. ISIE 2001. IEEE International Symposium on, 2001 pp. 661-665 vol.1.

[8] Clemente, S., Pelly, R. *Understanding power mosfet switching performance*. Solid State Electronics. Vol.26, n.12. 1983.

[9] Grant, D., Gowar, J. Power Mosfet: Theory and Applications. Wiley InterScience Publication. 1989. pp. 97-147. ISBN0-471-82867-X

[10] Mohan, N. Undeland, T.M., Robbins, W. Power Electronics. John Wiley and Sons, Inc. 1995. pp.581-593. ISBN: 0-471-58408-8

[11] Hertz, E.M., et al. Analysis of the tradeoffs between thermal behavior and EMI noise levels in a boost PFC circuit. Industry Applications Conference, 2001. Thirty-Sixth IAS Annual Meeting. Conference Record of the 2001 IEEE, Oct 2001 pp. 2460 -2465 vol.4.

[12] Takizawa, S. et al. A new di/dt control gate drive circuit for IGBTs to reduce EMI noise and switching losses. Power Electronics Specialists Conference, 1998. PESC 98 Record. 29th Annual IEEE, May 1998 pp. 1443 -1449 vol.2.

[13] Castaldo, F.C. et al. Implementation of an Integrated DC-DC Converter using CMOS Standard Technology and employing Smart Power Principles. Proceedings COBEP 2001. Florianópolis. 2001

[14] Allen, P., E., Geiger, R.L., Strader, N.R. Design Techniques for Analog and Digital Circuits. McGraw Hill. 1990. pp.143-167

[15] Cisper-22. Information Technology Equipment-Radio disturbance characteristics.-Limits and Methods of Measurements. International Electrotechnical Commission. 1997.

[16] Tanaka, M. et al. Measurements of Electromagnetic Noise Radiating from a Printed Line Model Driven by a Switching Device. IEICE Trans. Communication, Vol. E-80-B. Nov. 1997.

[17] Hewlett-Packard. Cookbook for EMC Pre-compliance measurements. Application Note.

[18] Paul, C. Introduction to Electromagnetic Compatibility. John Willey and Sons, INC. ISBN 0-471-54927-4.